ELSEVIER

Thermochimica Acta 400 (2003) 153–163

thermochimica acta

www.elsevier.com/locate/tca

Evidence of lanthanum–chromium mixed oxides formed in CrO_x/La_2O_3 model catalysts

D.L. Hoang [a,*], A. Dittmar [a], M. Schneider [a], A. Trunschke [a], H. Lieske [a], K.-W. Brzezinka [b], K. Witke [b]

[a] *Institute for Applied Chemistry Berlin-Adlershof, Richard-Willstätter-Str. 12, D-12489 Berlin, Germany*
[b] *Federal Institute for Materials Research and Testing (BAM), Richard-Willstätter-Str. 11, D-12489 Berlin, Germany*

Received 9 April 2002; received in revised form 19 September 2002; accepted 24 September 2002

Abstract

CrO_x/La_2O_3 mixed oxides, prepared by impregnating La_2O_3 with appropriate aqueous solutions of $(NH_4)_2CrO_4$ and calcining at 600 °C for 4 h, have been investigated by means of XRD, TPR, XPS, DRIFTS, and Raman spectroscopy (RS). The formation of the compounds La_2CrO_6, $La(OH)CrO_4$ and $LaCrO_4$ under these conditions was evidenced. Strong peaks at 864, 884, 913, and 921 cm^{-1}, as well as weak peaks at 136, 180, 354, 370, and 388 cm^{-1} in the RS spectrum of CrO_x/La_2O_3 have been assigned to La_2CrO_6.

Keywords: Lanthanum–chromium mixed oxides; La_2CrO_6; $LaCrO_4$; TPR; XPS; XRD; DRIFTS; Raman spectroscopy

1. Introduction

It is known that solid-state reactions of chromium(III) or chromium(VI) oxides with lanthana under certain conditions can lead to the formation of mixed oxide compounds, like $La_2(CrO_4)_3$, $LaCrO_4$ [1,2] and/or La_2CrO_6 [3]. By reduction, these mixed oxides are converted into perovskite type $LaCrO_3$, which has extensively been investigated as material for solid oxide fuel cells or as combustion catalyst (e.g. [3–5]). Recently, we have studied $CrO_x/La_2O_3/ZrO_2$ catalysts, prepared by impregnating a $La(OH)_3/Zr(OH)_4$ mixture with an aqueous solution of $(NH_4)_2CrO_4$ followed by calcination in air at 600 °C for 4 h. After reduction, these materials catalyze the dehydrocyclization of C_{6+} hydrocarbons to alkyl aromatics fairly selectively [6]. Our studies have revealed a stabilizing effect of lanthana on chromium oxide, enhancing its surface dispersion on zirconia and, therefore, the catalyst stability and regenerability [7]. The question arose, whether this stabilizing effect consists in the formation of lanthana–chromia surface compounds. To clarify this question, we have examined (i) whether and which lanthana–chromia mixed oxide compounds could be formed in a CrO_x/La_2O_3 mixed oxide system prepared as model catalysts at the conditions used in [6,7] for preparing the $CrO_x/La_2O_3/ZrO_2$ catalysts and (ii) the possibility of forming such compounds on the zirconia surface in $CrO_x/La_2O_3/ZrO_2$ catalysts.

In this paper we report the characterization results obtained by XRD, TPR, XPS, FTIR and Raman spectroscopy (RS) carried out on CrO_x/La_2O_3 model catalysts.

* Corresponding author. Fax: +49-30-6392-4370.
E-mail address: hoang@aca-berlin.de (D.L. Hoang).

0040-6031/03/$ – see front matter
PII: S0040-6031(02)00491-4

Table 1
Cr content, CrO_x/La_2O_3 molar ratio, BET surface and pore radius (PR) of the investigated samples

Samples	Cr content (wt.%)	Cr_2O_3/La_2O_3 molar ratio	BET (m^2/g)	PR (Å)
S1 (La_2O_3)	–	–	1.1	–
S2 (Cr_2O_3)	–	–	30.9	40.7
S3 ($LaCrO_3$)	21.8	–	2.5	41.8
S4 ((29)CL)	29.0	1.6	2.5	41.8
S5 ((1.0)CL)	1.0	0.03	14.6	38.9
S6 ((2.1)CL)	2.1	0.06	10.4	41.9
S7 ((4.1)CL)	4.1	0.13	8.6	41.5
S8 ((8.1)CL)	8.1	0.18	7.9	42.3

2. Experimental

2.1. Sample preparation

The investigated samples designated as S1–S8 are listed in Table 1. The samples S1–S4 were used as reference materials and S5–S8 as model catalysts. Below, the preparation and/or pretreatment conditions of all materials investigated are given in detail.

(S1) Commercially available lanthana (Fluka) has been pretreated by calcination in air at 600 °C for 4 h.

(S2) The product of the thermal decomposition of $(NH_4)_2CrO_4$ was prepared by dissolving the chromium precursor, $(NH_4)_2CrO_4$, in distillated water. The solution was kept at pH 10 by $(NH_4)OH$ addition. After evaporating the solvent at 50–60 °C, the product obtained has been calcined in air at 600 °C for 4 h.

(S3) $LaCrO_3$ has been synthesized through combustion reactions at 500 °C, using $La(NO_3)_3{\cdot}6H_2O$ and $Cr(NO_3)_3{\cdot}9H_2O$ as precursors and $CO(NH_2)_2$ as fuel [8]. The obtained product was calcined at 100 °C for 5 h.

(S4)–(S8) CrO_x/La_2O_3 model catalysts have been prepared by immersing lanthana, S1, into aqueous solutions containing the appropriate amounts of $(NH_4)_2CrO_4$. By ammonia addition, the solutions were kept at pH 10. Under stirring, the excess water was slowly evaporated at 50–60 °C. The products obtained were dried in air at 120 °C for 12 h, and calcined at 600 °C for 4 h, resulting in lanthana with different chromium loadings. The sample S4 contains 29.0% Cr and the Cr_2O_3/La_2O_3 molar ratio in S4 nearly corresponds to that of the 4% Cr/7% La_2O_3/ZrO_2 catalyst [6,7]. Below, the CrO_x/La_2O_3 model catalysts will be denominated as (*x*)CL, cf. Table 1, where *x* indicates the chromium loading (wt.%), C stands for chromium oxide and L for lanthana.

The specific surface areas and porosities of the materials under consideration have been determined after calcination, using a BET surface area analyzer NOVA-1200 (Quantachrome). The results are summarized in Table 1.

2.2. Characterization

X-ray powder diffraction (XRD) measurements were carried out on an STOE STADI P automated transmission diffractometer with Cu $K\alpha_1$ radiation at room temperature. The XRD pattern was scanned in 2θ range of 5–60° (step size 0.5°, 100 s per step) recorded with a position sensitive detector (PSD). The phase analysis was carried out with Visual X^{pow} program package, using the powder diffraction file (PDF) of the International Centre of Diffraction Data (ICDD).

Temperature programmed reduction (TPR) experiments have been performed using a gas flow system, including a fixed-bed quartz reactor and a gas analyzer unit. The calcined samples, with a particle size of 0.3–0.8 mm, were placed into the reactor and heated in an argon flow at 300 °C for 1 h before TPR. After cooling the sample in the argon flow to 50 °C, a TPR run was carried out in a 5.23% hydrogen in argon flow with a heating rate of 10 °C/min and at a gas flow rate of 15 ml/min. Optimum sample weights have been estimated according to Monti and Baiker [9]. Hydrogen consumed during TPR run was monitored by a thermal conductivity detector (GOW-MAC Instruments).

Assuming the Cr species in calcined samples were of the valence VI or V and in reduced sample—of the valence III, the hydrogen consumption, given as mmol H_2/g_{cat}, expected for the reduction of Cr(VI) to

Cr(III) and of Cr(V) to Cr(III) have been calculated by

$$Cr^n + [\tfrac{1}{2}(n-3)]H_2 \Leftrightarrow Cr^3 + (n-3)H^+ \quad (1)$$

with $n = 6$ or 5, respectively.

X-ray photoelectron spectra (XPS) were recorded on a SAGE 100 spectrometer (SPECS) using a non-monochromatized Mg Kα source operating at 20 mA and 12.5 kV. The La $3d_{5/2}$ peak of La_2O_3 at 835.1 eV was used as reference. The peaks were fitted with Gauss–Lorentz curves. For quantitative analysis, the peak areas were determined with a SPECS software after subtracting a Shirley background. The ratios I_{Cr}/I_{La}, calculated from the normalized intensities of the Cr $2p_{3/2}$ and La $3d_{5/2}$ peaks, were taken as a measure of the relative near-surface Cr concentrations in the CL samples.

Diffuse reflectance infrared transform (DRIFT) spectra were recorded on a spectrometer FTS-60 A (BIO-RAD) accumulating 256 scans at 2 cm^{-1} resolution. The ex situ calcined samples were placed in the reaction chamber of a diffuse reflectance attachment (HARRICK) and treated in O_2/He flow (20 ml/min) at 550 °C for 1 h. The spectra were measured at 40 °C and presented in Kubelka–Munk mode referring to a KBr background spectrum.

Raman spectra (RS) were recorded with a DILOR-XY-Spectrometer (Dilor, Bensheim, Germany) equipped with a nitrogen cooled charge coupled device (CCD) camera as detector. The samples were excited using 514.5 nm radiation from an ILA 120 argon ion laser or the 633 nm line from a HNA 188 He–Ne laser (both, Carl Zeiss, Jena, Germany) with power levels up to 10 mW incident into the entrance optics. Micro-sampling (180° backscatter geometry) was accomplished with Olympus 50× objective with a numerical aperture of 0.75. With this objective, the laser beam focal point diameter was ca. 2 μm. That high lateral resolution allows to investigate individual particles of samples different in shape or color to find out parts of the sample enriched in one of the present components. Thus, it was possible to identify different components at higher reliability. Taking into account scattering losses inside of the spectrometer, 1 mW power level into the entrance optics corresponds to an irradiation density of about 10^4 W cm^{-1} at the sample. If necessary, it was ascertained by using lower laser power levels (up to 0.1 mW of the 633 nm laser line) in order to avoid any thermal effect of the laser. Wavenumbers are given with an accuracy of approximately ±2 cm^{-1}.

3. Results and discussion

3.1. XRD

The reference materials S1–S4 and the C_2O_3/La_2O_3 model catalysts S5–S8 were investigated by XRD. The diffractogramms are shown in Figs. 1 and 2, respectively.

In Fig. 1, the diffractogramms of S1–S4 show the phases La_2O_3 [10], Cr_2O_3 [11], $LaCrO_3$ [4,5,12], and $LaCrO_4$ [1,2,13], respectively. Cr_2O_3 in S2 is surely the product of $(NH_4)_2CrO_4$ decomposition at high-temperature. In S4, besides $LaCrO_4$, crystallites of Cr_2O_3 and $Cr(OH)CrO_4$ [14] have been found. Fig. 2 reveals that the phases of lanthanum hydroxide, $La(OH)_3$ [15], and lanthanum oxide carbonate, $La_2O_2(CO_3)$ [16], can be recorded in all of the samples S5–S8. The position of the strong $La(OH)_3$ peaks cover up the main peaks of La_2O_3, so it is not clear, whether crystallites of La_2O_3 also exist. In S5, probably due to the low Cr content, not any of the Cr–La phases have been found. However, beginning with sample S6, the phase of the basic chromate La_2CrO_6 with Cr at the oxidation state VI appears, the formation and structure of which were characterized by Berjoan et al. [3]. With the samples S6–S8, the peaks assigned to the phase $LaCrO_4$ [1,2,13], with Cr at the oxidation state V can be observed additionally.

Thus, the XRD results demonstrate that the Cr precursor $(NH_4)_2CrO_4$ with the high valence Cr(VI), is not stable during a calcination in air at 600 °C, i.e. at calcination temperature used for preparing $Cr_2O_3/La_2O_3/ZrO_2$ catalysts [6], and decomposes forming Cr_2O_3. But, in contrast to this, the calcination of the Cr precursor mixed with lanthana results in Cr–La compounds with Cr in the stable oxidation states VI and/or V.

3.2. TPR of CL

The TPR experiments were performed with the samples S1, S2 and S4–S8. The TPR profiles obtained are shown in Fig. 3.

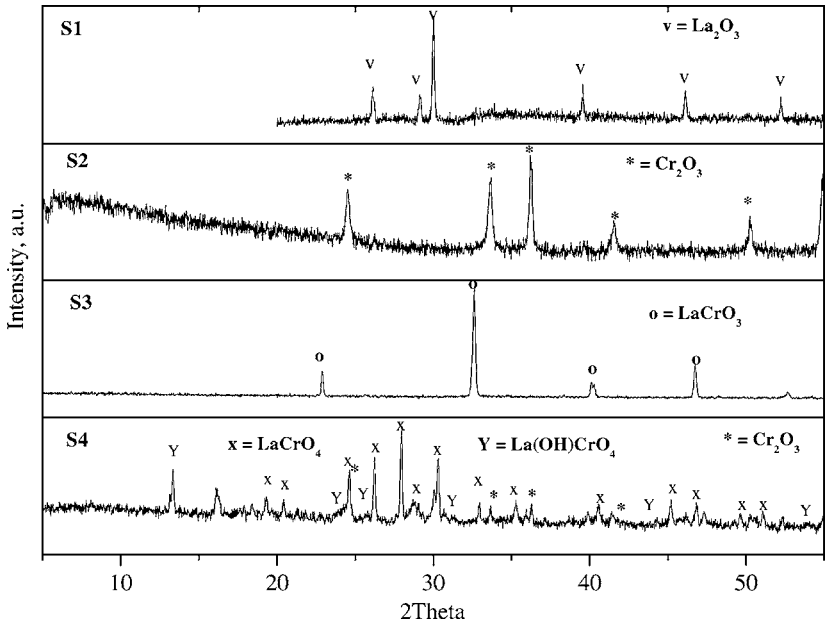

Fig. 1. XRD of samples S1–S4 (cf. Table 1): marks at some peaks stand for La_2O_3 (v), Cr_2O_3 (∗), $LaCrO_3$ (○), $LaCrO_4$ (x), $LaCr(OH)CrO_4$ (Y).

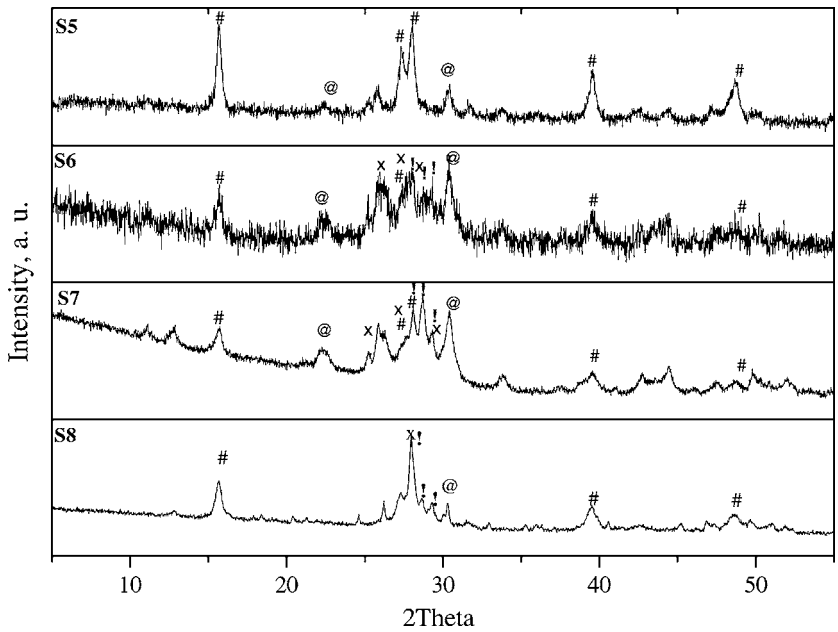

Fig. 2. XRD of samples S5–S8 (cf. Table 1): marks at some peaks stand for $La(OH)_3$ (#), La_2CrO_6 (!), $LaCrO_4$ (x), $La_2O_2CO_3$ (@).

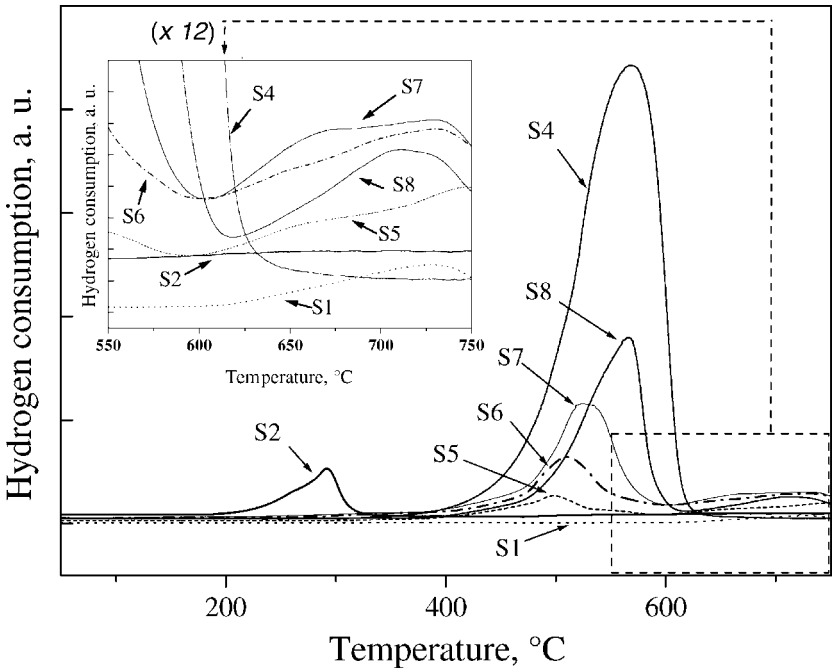

Fig. 3. TPR profiles of S2 and samples S4–S8 (cf. Table 1).

S1 consists of irreducible La_2O_3. Accordingly, during TPR of La_2O_3, no hydrogen consumption has been registered, with the exception of a broad peak at temperatures higher than 600 °C, which has been assigned by mass spectrometry to the reduction of carbon-containing surface contaminations. S2 consumes hydrogen in the temperature range between 200 and 300 °C, causing a broad peak with T_{max} = 292 °C. Since S2 mainly consists of irreducible Cr_2O_3 (as shown by XRD, cf. Fig. 1), this hydrogen consumption should be assigned to the reduction of surface Cr^{6+} species, partially formed after air treatment at 600 °C and anchored to the chromia lattice by Cr^{6+}–O_x bonds [17]. According to Eq. (1), the amount of Cr^{6+} has been estimated to be ca. 2.0 wt.%. The chromium-containing lanthana materials (S4–S8) exhibit two hydrogen consumption peaks, the first peak at lower temperatures with T_{max} in the temperature range between 400 and 600 °C and the second one at temperatures above 600 °C, see the magnified box in Fig. 3. Like with La_2O_3 (S1), the high-temperature peak observed with all lanthana-based samples, could be assigned to the reduction of surface carbon-containing species. The higher the chromium content, the higher is T_{max} of the low-temperature peak, namely 498, 510, 522, 566 and 570 °C for (1.0)CL, (2.1)CL, (4.1)CL, (8.1)CL and (29.0)CL, respectively. Since the intensity of this peak increases with increasing Cr loading and chromium is the only reducible component in this system, the peak should be assigned to hydrogen consumption by reduction of chromium oxide. The shift of T_{max} to higher values with increasing Cr loading indicates La–Cr-oxide interactions, which may lead to the formation of mixed oxide phases and, therefore, may inhibit the thermal decomposition of chromium species in oxidation states VI and/or V during calcination at 600 °C in air. Thus, the TPR results are in agreement with the XRD findings, which have evidenced the formation of mixed oxides in chromium-containing lanthana materials.

In the hydrogen containing argon flow of the TPR experiments, the Cr^{6+} and/or Cr^{5+} ions are expected to be reduced to Cr^{3+} ones [18]. The hydrogen consumption expected for the reduction of Cr(VI) to Cr(III) and for the reduction of Cr(V) to Cr(III), respectively, is depicted in Fig. 4 versus the Cr loading. The calculated hydrogen consumption has been compared with the

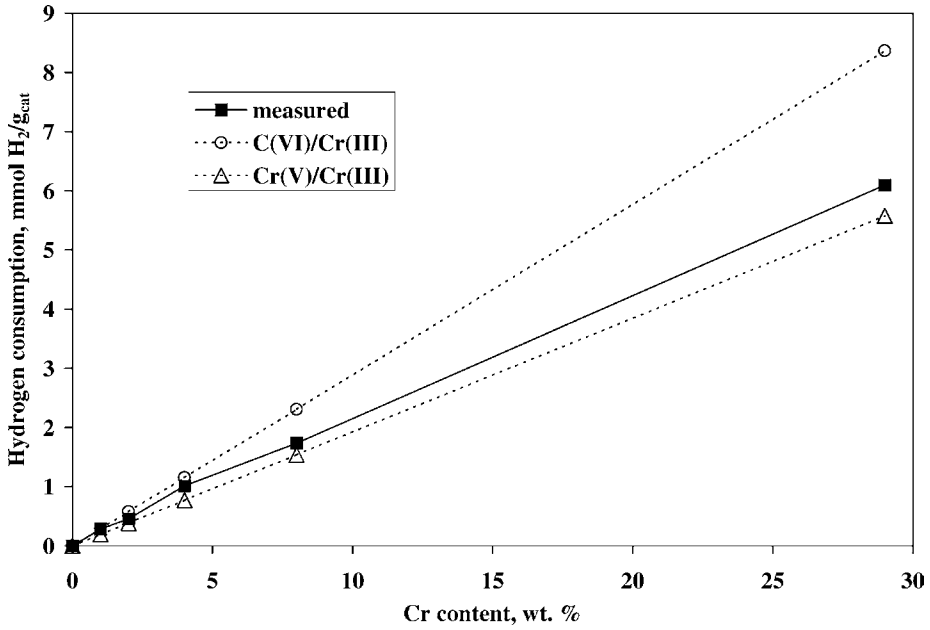

Fig. 4. Amount of hydrogen consumed during TPR on samples S4–S8 (cf. Table 1).

values measured in the TPR experiments with the samples S4–S8. The measured values are found to be lower than the calculated values of the Cr(VI) to Cr(III) reduction, but higher than the hydrogen consumption expected for the reduction of Cr(V) to Cr(III). The fact, however, that the measured curve of the samples with Cr loadings >8 wt.% more approximates to the calculated curve of the Cr(V) to Cr(III) reduction, suggests that, in calcined CL samples with chromium loadings higher than 8 wt.%, Cr(V) predominates among the fraction of the reducible chromium species.

3.3. XPS

Evidence on the oxidation state of chromium in the calcined samples has been obtained from XPS measurements. The XPS spectra obtained on S2–S4 (Cr_2O_3, $LaCrO_3$ and (29.0)CL) as well as on S1, S5–S8 (La_2O_3, (1.0)CL, (2.1)CL, (4.1)CL and (8.1)CL) samples (cf. Table 1), are depicted in Figs. 5 and 6, respectively.

In Fig. 5, the main peaks in the XPS spectra of the calcined samples S2 and S3 exhibit a binding energies of 576.4 and 575.8 eV, respectively, which are characteristic for Cr(III). This is in agreement with the XRD results showing Cr_2O_3 and $LaCrO_3$ as the main phases in S2 and S3, respectively. With these two samples, peak fitting reveals a shoulder at higher binding energies, representing Cr^{n+}, $3 < n < 6$. This is in agreement with the TPR results that revealed the traces of Cr(VI) and/or Cr(V) in samples S2, cf. Fig. 3, and S3 (not shown here). The main peak in the XPS spectrum of S4 shows a binding energy of 578.8 eV, which can be assigned to Cr(V). This confirms the XRD and TPR findings revealing the formation of $LaCrO_4$ with Cr in oxidation state (V). Moreover, the peak fitting reveals, in accordance with the XRD analysis, the presence of a minor fraction of Cr species with binding energies smaller than 577.0 eV, characteristic for Cr in lower oxidation states, e.g. Cr_2O_3 (cf. Fig. 1).

In Fig. 6, the XPS spectra of the samples S5–S8 exhibit Cr $2p_{3/2}$ peaks with a binding energy of 579.9 eV. The interpretation of this peak is complicated by the fact that La_2O_3 usually shows a shake-up satellite of oxygen on the high binding energy side of the O 1s signal, which can affect the chromium signals [19]. Therefore, a spectrum of La_2O_3, S1, was recorded in the Cr $2p_{3/2}$ region, too. As shown in Fig. 6, the O 1s satellite of La_2O_3 appears at a binding energy of

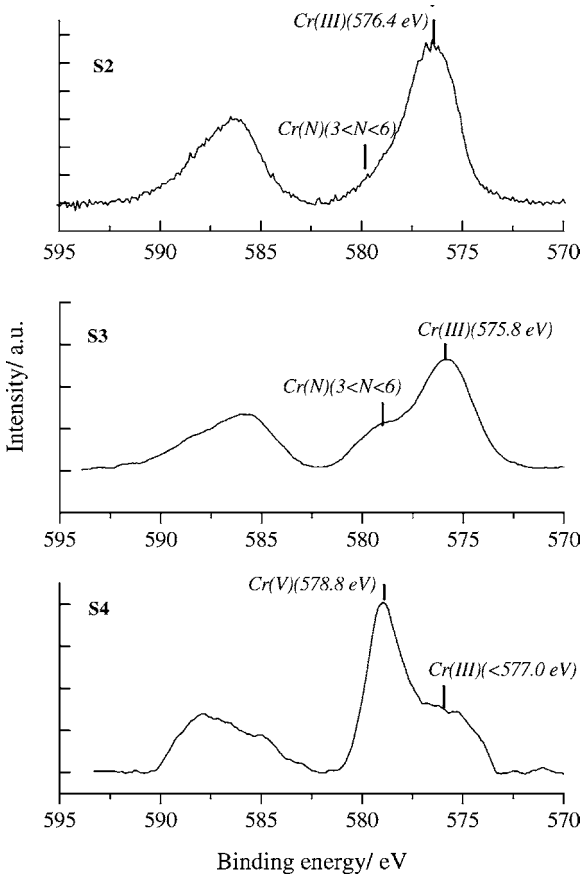

Fig. 5. XPS spectra of calcined samples S2–S4 (cf. Table 1).

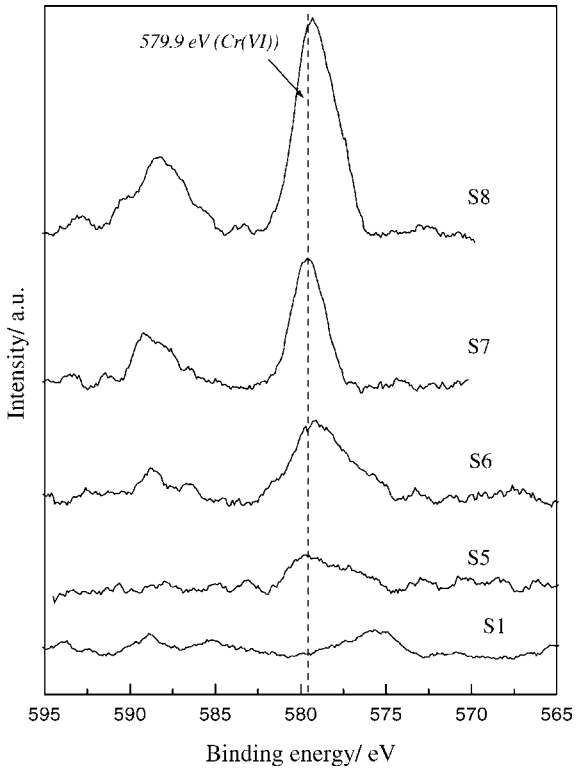

Fig. 6. XPS spectra of lanthana (S1), and CL samples (S5–S8, cf. Table 1).

575.5 eV. However, it was not detected in spectra of the samples S5–S8. Therefore, the peak at 579.9 eV can reliably assigned to Cr(VI) [7]. The higher the chromium loading, the higher is the intensity of this Cr $2p_{3/2}$ peak. Since this peak is partly broadened, however, the coexistence of another high valence Cr^{n+} species, $3 < n < 6$, cannot be excluded.

The intensity ratios of the Cr $2p_{3/2}$ and La $3d_{5/2}$ peaks, I_{Cr}/I_{La}, representing the relative near-surface concentration of Cr species, are presented in Table 2 as a function of the Cr loading. For Cr loadings lower than 2 wt.%, the I_{Cr}/I_{La} ratio drastically increases with increasing Cr loading. With the Cr loadings >2 wt.%, the I_{Cr}/I_{La} ratios remains almost constant. This observation suggests sintering of Cr species on the La_2O_3 surface and/or on an incorporation of chromium into the bulk.

To summarize, in agreement with the TPR experiments, XPS measurements show that Cr(VI) and Cr(V) are the predominating oxidation states of chromium in the calcined CrO_x/La_2O_3 model catalysts.

3.4. DRIFT spectroscopy

In Fig. 7, DRIFT spectra of the samples S1 and S4–S7 are compared in the O–H stretching region.

Table 2
Intensity ratios of the Cr $2p_{3/2}$ and La $3d_{5/2}$ peaks, I_{Cr}/I_{La}, representing the relative near-surface concentration of Cr species, as a function of Cr loading (wt.%)

Sample	Cr loading (wt.%)	I_{Cr}/I_{La}
S5	1.0	0.09
S6	2.1	0.16
S7	4.1	0.14
S8	8.1	0.18

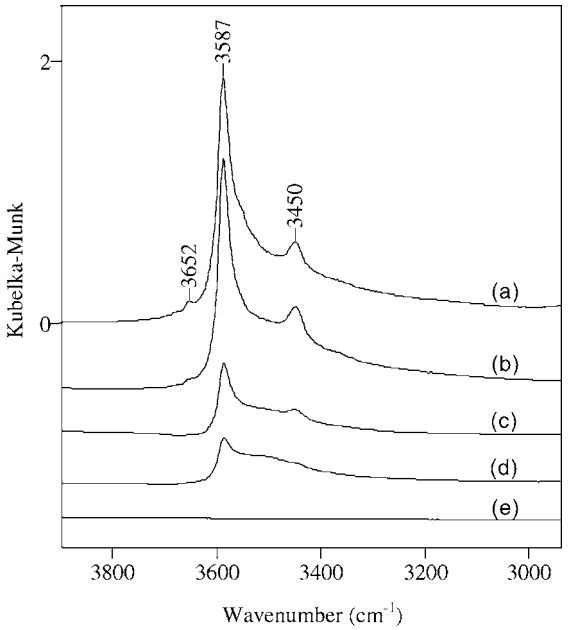

Fig. 7. DRIFT spectra of the samples S1 (a), S5 (b), S6 (c), S7 (d) and S4 (e) (cf. Table 1) in the O–H stretching region.

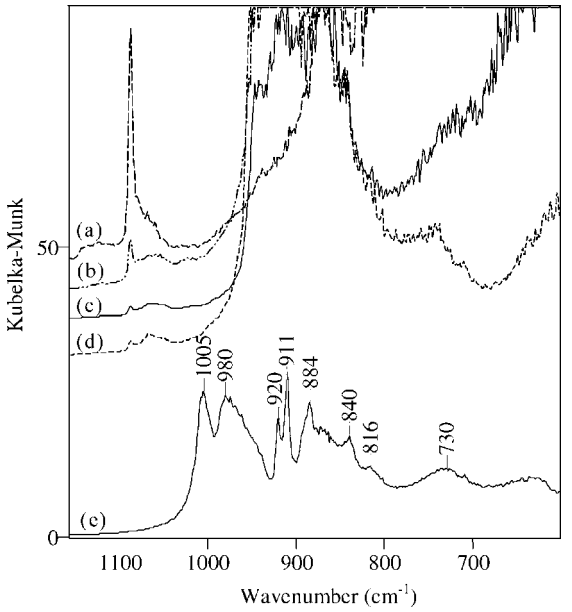

Fig. 8. DRIFT spectra of the samples S1 (a), S5 (b), S6 (c), S7 (d) and S4 (e) (cf. Table 1) in the Cr=O and Cr–O stretching region.

Before measurement, the materials were calcined in situ at 550 °C. The spectrum of lanthana reveals bands at 3587, 3450 and 3652 cm^{-1}. These bands are consistent with bulk and surface hydroxyls of lanthanum hydroxide and lanthanum oxide. The strong OH band at 3587 cm^{-1} is attributed to $La(OH)_3$ [20]. Oxyhydroxide (LaOOH), which is formed during the first step of $La(OH)_3$ dehydration, is characterized by the OH band at 3450 cm^{-1} [20,21]. The weak band at 3652 cm^{-1} is assigned to isolated terminal La–OH groups on the surface of La_2O_3 [22,23]. The intensities of all these hydroxyl stretching bands are observed to decrease upon chromium oxide addition. In the infrared spectrum of the sample S4, containing mainly $LaCrO_4$ compound, not any La–OH band was detected. This finding shows, in accordance with the common view of the mechanism of chromium anchoring on oxide surfaces [18], that the lanthanum hydroxyl groups are involved in an acid–base reaction with Cr^{6+} species, resulting in anchored chromate structures. This seems plausible, because, if La_2O_3 powder is immersed in water or in an aqueous solution during the sample preparation procedure described above, cf. Section 2, it reacts to form an insoluble hydroxide [24], which may readily react with CrO_4^{2-} ions. The reaction of La_2O_3 with water may change the morphology of the particles, increasing their surface area. In fact, an increase of specific surface area has been really observed with data presented in Table 1, from 1.1 m^2/g for S1 (La_2O_3) to 14.6 m^2/g for S5 ((1.0)CL).

Chromium–oxygen groups show stretching bands in the 1050–830 cm^{-1} region. For (1.0)CL, (2.1)CL and (4.1)CL, a detailed interpretation of the Cr=O and Cr–O stretching vibrations is not possible due to the very low reflection in this region, see Fig. 8. Resolved overtone and combination bands were also not observed, indicating a considerable heterogeneity of the corresponding chromium surface compounds. The sharp peak at 1088 cm^{-1} in the spectra of La_2O_3, (1.0)CL, (2.1)CL and (4.1)CL is attributed to a lanthanum carbonate species. The DRIFT spectrum of (29.0)CL shows bands at 1005, 980, 950 (shoulder), 920, 911, 884, 840, 816, and 730 cm^{-1}. As shown above, XRD revealed the formation of a $LaCrO_4$ phase in this sample. The transmission spectrum of $LaCrO_4$, dispersed and pressed in KBr, was reported to be characterized by bands at 935, 830, 800 and 720 cm^{-1} [25]. Consequently, the shoulder near 950 cm^{-1} and

the bands at 840, 816 and 730 cm^{-1} in the DRIFT spectrum of (29.0)CL might be interpreted in terms of $LaCrO_4$. The $LaCrO_4$ bands, however, overlap with spectral features of other chromium species. The stretching mode of Cr–O–Cr chains at 884 cm^{-1} indicates the presence of polymeric chromium complexes. The four bands at 1005, 980, 920 and 911 cm^{-1} are attributed to Cr=O stretching vibrations of mono- and polynuclear surface chromates. Bands due to $LaCrO_3$ [26] and Cr_2O_3 [27] in the 700–400 cm^{-1} region were not observed.

3.5. Raman spectroscopy

RS is a powerful characterization technique for studying supported chromium oxide catalysts because it can differentiate between various molecular states of oxide species [18,19]. In this work, RS was used for investigating the mixed oxide samples S5 ((1.0)CL), S6 ((2.1)CL) and S7 ((4.1)CL) with a lateral resolution of about 2 μm in order to identify possible compounds formed therein after air treatment at 600 °C for 4 h. Identification of those compounds is either based on the comparison of the sample spectra with data already published or, in some cases, on their identity ascertained by our corresponding XRD studies.

RS spectra of source or other relevant materials, $La(OH)_3$, La_2O_3 and Cr_2O_3 are shown in Fig. 9. They

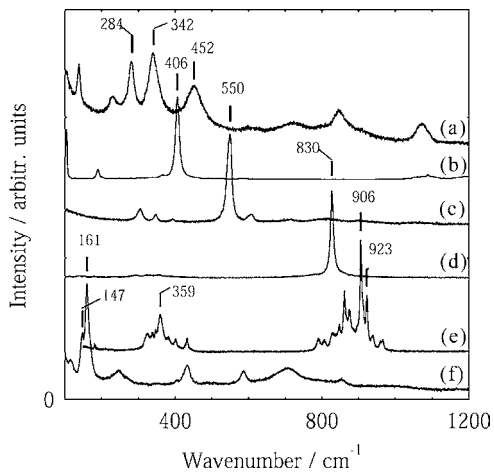

Fig. 9. Raman spectra of some La/Cr reference compounds: (a) $La(OH)_3$, (b) La_2O_3, both containing traces of $La_2(CO_3)_3$, peaks at ca. 1080 cm^{-1}, (c) Cr_2O_3, (d) $LaCrO_4$, (e) $La(OH)CrO_4$ and (f) $LaCrO_3$. Spectra are vertically shifted for clarity.

are well known and reported elsewhere. The spectrum of lanthanum hydroxide, $La(OH)_3$ (a), exhibits six peaks at 140, 234, 284, 342, 452 and 600 cm^{-1} [28] and the one of crystalline La_2O_3 (b) shows three sharp peaks at 105, 192 and *406* cm^{-1} (italicized: strongest peaks) [28,29]. The Cr_2O_3 single crystal spectrum (c) exhibits six peaks at 303, 351, 397, 530, *550* and 609 cm^{-1} with dominating relative intensity of the 550 cm^{-1} peak for most orientations of the crystal [30] as well as in the spectra of powders. Crystalline bulk CrO_3 as species in general does not play any role in supported chromium-based catalysts. Its spectrum is dominated by a peak at 970 cm^{-1} [31].

The spectra of $LaCrO_4$ and $NdCrO_4$ containing chromium in the valence state (V) have been recently reported for the first time [32]. In agreement with XRD result showing the formation of $LaCrO_4$ phase in S4, cf. Fig. 1, peaks at 232, 239, 304, 334, 384 and *830* cm^{-1} in the RS spectrum of S2 must be assigned to $LaCrO_4$ (cf. Fig. 8, spectrum (d)). However, S4 is not a pure phase. The heterogeneous S4 sample relatively often supplies spectra showing many peaks in the 300–450 and 800–950 cm^{-1} spectral ranges, strongest of them are positioned at 359, 906 and 923 cm^{-1} (Fig. 9, spectrum (e)). Peak positions and relative intensities are very similar to the spectrum of the $Er(OH)CrO_4$ compound [33], but differs somewhat from the published one of $La(OH)CrO_4$ [34]. More detailed investigations show this is sensitive against warming by laser radiation. Spectra obtained by higher laser power levels show broadened peaks shifted to lower wavenumbers, for instance from 904 cm^{-1} of the strongest peak for 0.5 mW to 898 cm^{-1} for 2.5 mW (514 nm radiation, respectively). The process is reversible in a certain degree. Possibly, thermal effects are the reason for differences in published data. A spectrum obtained of a $La(OH)CrO_4$ part of the S4 sample by an exciting laser levels of 0.5 mW of the 633 nm radiation exhibit peaks at 324, 339, 347, *359*, 382, 401, 432, 790, 807, 829, 847, *861*, *874*, *906*, *923*, 939, 959 and 966 cm^{-1}. The presence of the $La(OH)CrO_4$ phase in the S4 sample is also confirmed by XRD results, cf. Fig. 1.

The dominating phase in the sample S3 is ascertained by XRD as the perovskite like material $LaCrO_3$, cf. Fig. 1. For comparison, its RS spectrum is also depicted in Fig. 9, see spectrum (f). In contrast to the spectra of La_2O_3 and Cr_2O_3, the one of S3 does not

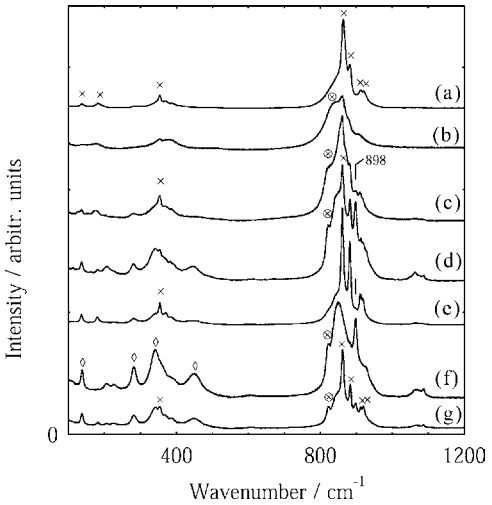

Fig. 10. Raman spectra of lanthanum–chromium mixed oxides (a) and (b) S7, (c)–(e) S6 and (f) and (g) S5 (cf. Table 1); marks at some peaks stand for $La(OH)_3$ (◇), La_2CrO_6 (×) and $LaCrO_4$ (⊗), respectively. Spectra are vertically shifted for clarity.

show its strongest peak suited for indication in the region of Me–O valence vibrations (Me = La, Cr), but at 147 and 161 cm^{-1} in the range of lattice vibrations.

Using the RS spectra presented in Fig. 9 as the reference ones we examined the RS spectra obtained for different particles of S7, S6 and S5 samples (cf. Section 2) and depicted in Fig. 10(a)–(g), respectively. As appeared, the spectra of the sample S7, (4.1)CL, (Fig. 9(a) and (b)) exhibit weaker peaks at 136, 180, 354, 370 and 388 cm^{-1} as well as stronger ones at *864*, *884*, 913 and 921 cm^{-1}. According to the XRD result shown in Fig. 1, in S7 the phases of $La(OH)_3$, of the basic chromate La_2CrO_6 and, probably, of La_2O_3 exist. So, keeping in mind that hydroxide $La(OH)_3$ exhibits six peaks at 140, 234, *284*, *342*, *452* and 600 cm^{-1}, see Fig. 9(a), and crystalline La_2O_3—three sharp peaks at 105, 192, and *406* cm^{-1}, see Fig. 9(b), the RS spectrum observed for S7 in Fig. 10(a) and (b) should be assigned to basic chromate La_2CrO_6. A similar feature shows the spectrum of the chromate of an other trivalent cation, $Al_2(CrO_4)_3{\cdot}H_2O$, with the peaks at 352 and *865* cm^{-1} [35].

Based on the reference spectra presented in Fig. 9 and on the assignment made above for the sample S7, we examined the further RS spectra recorded for some different particles of the mixed lanthanum–chromium oxide powders S5 ((1.0)CL) and S6 ((2.1)CL). So, the RS spectra shown in Fig. 10(c)–(g) for both the samples evidence the existence of $La(OH)_3$, characterized by the peaks ranged from 140 to 600 cm^{-1}, and $LaCrO_4$—by the peak appeared as a shoulder at 830 cm^{-1}. This is in accordance with XRD results, cf. Fig. 2. But, some peaks at about 350, 864, 884, 913 and 921 cm^{-1}, marked as "x" in Fig. 10, clearly reveal that the CL samples also consist of changing parts of La_2CrO_6 as well as a little part of $La_2(CO_3)_3$, as known, usually characterized by the weak peaks at about 1070 cm^{-1}, see Fig. 10(d), (f) and (g). Moreover, a sharp band appears at 898 cm^{-1} in some RS spectra of S5 and S6 samples (cf. Fig. 10(d) and (f)). Further investigations show the 898 cm^{-1} position of that peak may be the result of warming of the sample (see above) and, thus, suggests the peak represents the $La(OH)CrO_4$ compound. In this case, RS is only qualified to detect little local enrichments of that phase because of its high lateral resolution of 2 μm. $La(OH)CrO_4$ could not be found in the S5 and S6 samples by XRD, probably, due to its low concentration.

In summary, the RS measurements reveal the formation of La_2CrO_6, $La(OH)CrO_4$ as well as $LaCrO_4$ in the CL model catalysts. This is in agreement with the TPR and XPS findings showing that the predominating oxidation states of chromium in the calcined CL materials are Cr(VI) and Cr(V). Since the CrO_x/La_2O_3 model catalysts were prepared at the conditions used for preparing $CrO_x/La_2O_3/ZrO_2$ catalysts, these findings strongly suggest that such lanthanum–chromium mixed oxides could also be formed as surface compounds on $CrO_x/La_2O_3/ZrO_2$ catalysts. Evidencing this and examining whether it could be a reason for the stabilizing effect of lanthana on chromia in these catalysts [7] will be the objectives of further investigations.

4. Conclusion

- The calcination of a dry $(NH_4)CrO_4/La_2O_3$ mixture, prepared by immersing La_2O_3 into an aqueous $(NH_4)CrO_4$ solution, at 600 °C for 4 h has been shown to lead to formation of mixed oxide compounds as La_2CrO_6, $LaCrO_4$ and $La(OH)CrO_4$. It is suggested that such lanthanum–chromium mixed oxides could also be formed as surface compounds on $CrO_x/La_2O_3/ZrO_2$ catalysts.

- The formation of those mixed oxide compounds may take place through an acid–base esterification of OH groups, formed on lanthana, by CrO_4^{2-} ions.
- For the first time, a Raman spectroscopic study reveals the RS spectrum of the compound La_2CrO_6 exhibiting the weaker peaks at 136, 180, 354, 370 and 388 cm^{-1} as well as the stronger ones at 864, 884, 913 and 921 cm^{-1}.

Acknowledgements

This work was supported by the Berlin Senat Department of Science, Research and Culture (project No. 89 11 30 001) as well as by the Federal Ministry of Education and Research of the Federal Republic of Germany (project No. 03C30120). The authors are grateful to Dr. S. Möhmel, Institute for Applied Chemistry Berlin-Adlershof, Berlin, Germany, for supplying the sample S3 ($LaCrO_3$) and Dr. J. Radnik, Institute for Applied Chemistry Berlin-Adlershof, Berlin, Germany, for useful discussions.

References

[1] H. Schwarz, Z. Anorg. Allg. Chem. 322 (1963) 1.
[2] A. Furusaki, H. Konno, R. Furuichi, Thermochim. Acta 253 (1995) 253.
[3] R. Berjoan, J.P. Traverse, J.P. Coutures, Rev. Chim. Minér. 10 (1973) 309.
[4] B. de Collonge, E. Garbowski, M. Primet, J. Chem. Soc., Faraday Trans. 87 (15) (1991) 2483.
[5] W. Zheng, W. Pang, G. Meng, D. Peng, J. Mater. Chem. 9 (1999) 2833.
[6] H. Lieske, D.L. Hoang, US Patent 6,239,323 B1.
[7] A. Trunschke, D.L. Hoang, J. Radnik, H. Lieske, J. Catal. 191 (2000) 456.
[8] D.A. Fumo, M.R. Morelli, A.M. Segadaes, Mater. Res. Bull. 31 (10) (1996) 1243.
[9] D.A.M. Monti, A. Baiker, J. Catal. 83 (1983) 323.
[10] International Centre of Diffraction Data (ICDD), PDF No. [74-1144].
[11] International Centre of Diffraction Data (ICDD), PDF No. [76-0147].
[12] International Centre of Diffraction Data (ICDD), PDF No. [33-0701].
[13] International Centre of Diffraction Data (ICDD), PDF No. [36-0093].
[14] International Centre of Diffraction Data (ICDD), PDF No. [84-1859].
[15] International Centre of Diffraction Data (ICDD), PDF No. [36-1481].
[16] International Centre of Diffraction Data (ICDD), PDF No. [84-1963].
[17] M.I. Zaki, N.E. Fouad, G.C. Bond, S.F. Tahir, Thermochim. Acta 285 (1996) 167.
[18] B.M. Weckhuysen, I.E. Wachs, R.A. Schoonheydt, Chem. Rev. 96 (1996) 3327.
[19] D. Brune, R. Hellborg, H.J. Whitlow, O. Hunderi (Eds.), Surface Characterization, Wiley/VCH, Weinheim, 1999.
[20] M.P. Rosynek, D.T. Magnuson, J. Catal. 46 (1977) 402.
[21] B. Klingenberg, M.A. Vannice, Chem. Mater. 8 (1996) 2755.
[22] A.A. Tsyganenko, J. Lamotte, J.P. Gallas, J.C. Lavalley, J. Phys. Chem. 93 (1989) 4179.
[23] S. Lacombe, C. Geantet, C. Mirodatos, J. Catal. 151 (1994) 439.
[24] J. Kirchnerova, D. Klvana, Solid State Ionics 123 (1999) 307.
[25] T. Kikkawa, M. Yoshinaka, K. Hirota, O. Yamaguchi, J. Mater. Sci. Lett. 14 (1995) 1071.
[26] M.V. Kuznetsov, I.P. Parkin, Polyhedron 17 (1998) 4443.
[27] R. Marshall, S.S. Mitra, P.J. Gielisse, J.N. Plendl, C.L. Mansur, J. Chem. Phys. 43 (1965) 2893.
[28] S.S. Chan, A.T. Bell, J. Catal. 89 (1984) 433.
[29] M. Scheithauer, H. Knözinger, M.A. Vannice, J. Catal. 178 (1998) 701.
[30] I.R. Beattie, T.R. Gilson, J. Chem. Soc. A (1970) 980.
[31] H. Siebert, Anwendungen der Schwingungsspektroskopie in der Anorganischen Chemie, 1st ed., Springer, Berlin, 1966, p. 120.
[32] Y. Aoki, H. Konno, H. Tachikawa, M. Inagaki, Bull. Chem. Soc. Jpn. 73 (2000) 1197.
[33] I. Bueno, C. Parada, R. Saez Puche, E.J. Baran, J. Alloys Comp. 225 (1995) 237.
[34] I. Bueno, C. Parada, R. Saez Puche, I.L. Botto, E.J. Baran, J. Less-Common Met. 169 (1991) 105.
[35] R.A. Nyquist, C.L. Putzig, M.A. Leugers, Handbook of Infrared and Raman Spectra of Inorganic Compounds and Organic Salts, vol. 2, Raman Spectra, Academic Press, San Diego, 1997, p. 143.